Failure criterion for timber beams loaded in bending, compression and shear

van der Put, TACM

Important note
To cite this publication, please use the final published version (if applicable).
Please check the document version above.

ORIGINAL ARTICLE

Failure criterion for timber beams loaded in bending, compression and shear

T. A. C. M. VAN DER PUT

Faculty of Civil Engineering and Geosciences, Timber Structures and Wood Technology, Delft University of Technology, PO Box 5048, NL-2600 GA Delft, The Netherlands

Abstract
Based on the elastic–plastic strength calculation, necessary for precise data explanation, a derivation is given of the failure criterion for combined bending, compression and shear. This exact limit state criterion should replace the unacceptable unsafe criteria of Eurocode 5 (EN 1995-1-1:2004). It is shown that the principle used thus far, of limited "flow" in axial compression as a determining failure criterion, for example, predicting no influence of a size effect, does not hold. Instead, it is derived and confirmed by the data that bending tension failure is always determining, showing the existence of a size effect, and correction of the existing calculation method is therefore necessary. Because of the primary importance of the size effect for the strengths, also for combined bending–compression, a simple derivation of the size effect design equations is given and discussed in an appendix.

Keywords: *Combined bending–compression–shear strength, failure criterion, limit analysis, timber.*

Introduction

In the 1970s, strength tests at the Delft Stevin laboratory for combined bending and compression demonstrated a volume effect leading to a follow-up programme on semi-full-scale glulam beams with the theoretically necessary perfect boundary conditions of the supports. Damage always occurred through lateral buckling following cracking sounds during loading and a decrease in the modulus of elasticity after unloading, even when the test was stopped at the smallest possible lateral displacements. This applies even for the most slender beams, applied in praxis, which were expected to remain elastic, suitable for further testing of multiload combinations. The theory of elasticity in Chen and Atsuta (1972) does not show bifurcation for the three-dimensional lateral buckling case, and the large displacements analysis (third order theory) shows a continuous rise in the loading curve. This means that the top of a loading curve always is due to damage and failure and therefore elastic buckling does not exist in praxis for structural elements. Stability design is a common second order strength

calculation. The solutions of the second order equilibrium equations have to satisfy the failure criterion. This failure criterion is therefore essential and has to be discussed first. As shown in van der Put (2009), for statically indeterminate structures, and here, for combined loading, in wood design the idealized linear elastic calculation applied for failure, as given by the dashed lines in Figure 1, is not sufficient to describe and predict strength behaviour and needs to be replaced by the elastic–plastic calculation (solid lines in Figure 1). The existing models and proposed design rules of the Eurocode 5 (2004) therefore have to be corrected in this way. At the moment three different criteria are prescribed in the Eurocode for basically the same strength calculation: $n^2 + m = 1$ (eq. 6.19), $n + m = 1$ (eq. 6.23) and $m^2 + n = 1$ (eq. 6.35), where n and m are the normalized real compression and bending loadings N/N_u and M/M_u relative to the ultimate compression strength N_u and bending strength M_u.

This needs to be replaced by one equation of the real failure criterion (eq. 5), which accounts for the elastic–plastic behaviour of wood, showing unlimited plastic flow in compression and brittle-like behaviour
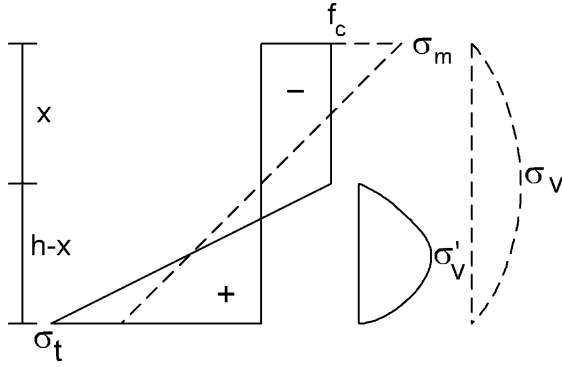
Figure 1. Bending and shear stress.

in tension (thus showing a volume effect for tension). The hypothesis of limited ultimate strain in compression followed so far is too conservative and has to be abandoned. Finite ultimate strain is not a material property but is caused by instability of the test. Limited strain was introduced for concrete in the 1960s by the parabolic stress diagram. It appeared that this diagram had to be extended by a full plastic range to be able to describe combined bending–compression failures. The same applies for steel and wood. The previous models for wood (e.g. Johns & Buchanan, 1982; Blass, 1987) are based on the principle of limited flow, leading to inconsistent adaptations that have to be corrected, especially because the Eurocode and other standards are based on this invalid restriction.

Derivation of the failure criterion for bending with compression and shear

The idealized elastic–plastic bending strength behaviour of wood (Figure 1), based on plasticity theory, provides the highest lower bound of the strength of limit analysis. The description is therefore the closest to the exact solution and close to the actual behaviour and measurements, and thus is able to predict behaviour. The equilibrium equations of this beam with width b and height h, loaded by a moment M, normal force N and shear force V are, according to Figure 1:

$$\frac{M}{b} = \frac{\sigma_c - \sigma_t}{2}(h-x)\left(\frac{h}{2} - \frac{h-x}{3}\right) \tag{1}$$

$$\frac{N}{bh} = \sigma_c - \frac{\sigma_t + \sigma_c}{2}\left(1 - \frac{x}{h}\right) \tag{2}$$

Because the bending tension strength $\sigma_t = f_t$ is normally higher than the compression strength due to the volume effect, flow in compression occurs, or $\sigma_c = f_c$, and elimination of x/h from eq. (1) and eq. (2) gives:

$$\frac{6M}{bh^2} = f_c\left(1 - \frac{N}{bhf_c}\right)\left(\frac{-1 + 3\sigma_t/f_c + 4N/bhf_c}{1 + \sigma_t/f_c}\right) \tag{3}$$

For bending only, when $N = 0$, this is:

$$\sigma_m = \frac{6M}{bh^2} = f_c\frac{3\sigma_t/f_c - 1}{\sigma_t/f_c + 1} = f_c\frac{3s - 1}{s + 1} \tag{4}$$

where σ_m is the apparent linear elastic bending stress (Figure 1) and $s = \sigma_t/f_c$. For combined compression bending failure, the tensile strength is reached: $\sigma_t = f_t$, $\sigma_m = f_m$ and $s = f_t/f_c$. From eqs (3) and (4) then follows:

$$\frac{6M}{f_m bh^2} = \frac{M}{M_{u,a}} = \left(1 - \frac{N}{N_u}\right)\left(1 + \frac{4N/N_u}{3s - 1}\right) \tag{5}$$

where $M_{u,a} = f_m bh^2/6$ is the apparent linearized bending strength and $N_u = f_c bh$ is the pure compression strength. For high values of s (high-quality material), eq. (5) becomes:

$$M/M_{u,a} \approx 1 - N/N_u \tag{6}$$

the failure criterion of most Regulations and also of the Eurocode, where it applies for columns only. For $s = 1.67$, eq. (5) becomes:

$$M/M_{u,a} = 1 - (N/N_u)^2 \tag{7}$$

the unsafe criterion of the Eurocode applying there for beams only.

According to Figure 1, the shear force V for failure is, when $\sigma_v' = f_v'$ and thus when the apparent linearized elastic shear stress $\sigma_v = f_v$:

$$V_u = \frac{2}{3}f_v'\left(1 - \frac{x}{h}\right)bh = \frac{2}{3}f_v bh$$

$$= \frac{2}{3}f_v' bh\frac{2}{s+1}\left(1 - \frac{N}{N_u}\right) \tag{8}$$

when eq. (2) is substituted.

For $N = 0$, the shear strength is $V_u = V_{u,0}$ and eq. (8) can be written:

$$\frac{V}{V_{u,0}} = \left(1 - \frac{N}{N_u}\right) = \frac{M}{M_{u,a}}\frac{a_c}{a} = \frac{M}{M_{u,a}}\frac{3h}{a} \tag{9}$$

where $a/h = M/Vh$ is the shear slenderness with a critical value of:

$$a_c/h = M_{u,a}/V_{u,0}h$$

$$= \sigma_m(bh^2/6)/\{(2/3)bh^2 f_v\} = f_m/(4f_v) \tag{10}$$

Equation (9) is a straight line, giving a cut-off of the parabolic Eurocode criterion eq. (7), as discussed below, showing also that the critical value of a is $a_c = 3h$.

Parameter estimation

As for the discussed models, the data of Johns and Buchanan (1982) are used here for parameter estimation of eq. (5). Each point of Figures 2–5 represents test results of 100 boards of 89×140 mm lumber of
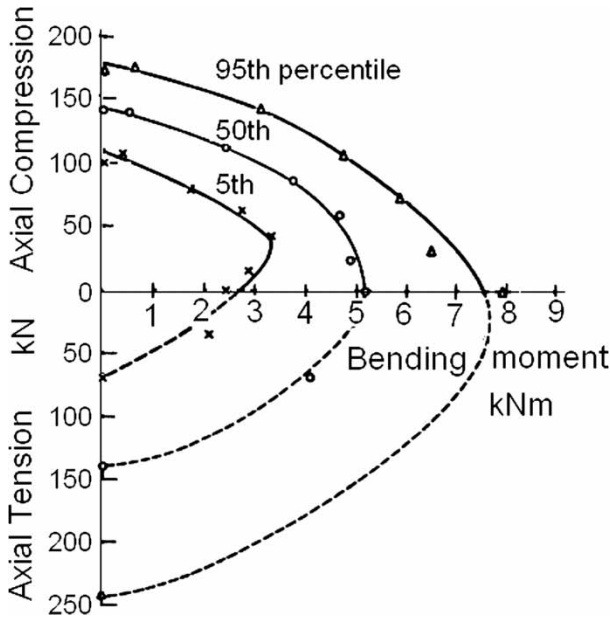
Figure 2. Combined bending–compression and bending–tension strength.

the spruce–pine–fir species group of grade 2 and better, kiln dried. The data are given in Figure 2. Because the nominal scale is not right, only normalized quantities are used. Equation (5) will be written:

$$m = 1 - n + \frac{4n - 4n^2}{3s - 1} \qquad (11)$$

where $m = M/M_{u,a}$ and $n = N/N_u$.

Trials show that:

- for the 95th percentile, $s = 2$ and eq. (11) becomes $m = 1 - 0.2n - 0.8n^2$
- for the 50th percentile, $s = 1.3$ and eq. (11) becomes $m = 1 + 0.38n - 1.38n^2$
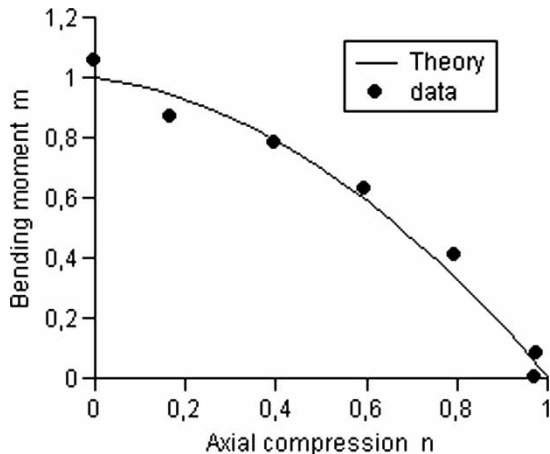- for the 5th percentile, $s = 0.77$ and eq. (11) becomes $m = 1 + 2.05n - 3.05n^2$.

Figure 3. $s = 2$ or 95th percentile of the bending–compression strength.
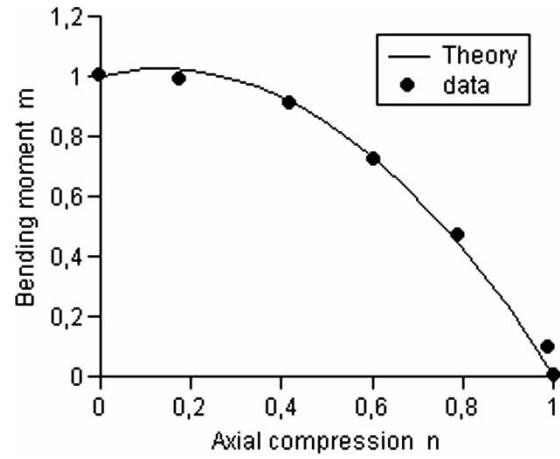

Figure 4. $s = 1.3$ or 50th percentile of the bending–compression strength.

The plots of these equations are given in Figures 3–5, respectively.

A higher value than $s = 1.3$ is necessary to fit the data for combined bending with tension. The sketched mean strength line of Figure 2, the parabolic failure criterion of the Eurocode 5, shows a maximum of m of eq. (11) at $n = 0$. Thus:

$$\frac{\partial m}{\partial n} = \frac{\partial}{\partial n} \left(1 - n + \frac{4n - 4n^2}{3s - 1} \right) = \left(-1 + \frac{4 - 8n}{3s - 1} \right)_{n=0}$$

$$= -1 + \frac{4}{3s - 1} = 0$$

(12)

giving $s = 5/3 = 1.67$. A higher value is to be expected for glulam as follows, from a Delft students' project of lateral–torsional buckling by bending with axial compression on semi-full-scale beams with perfect boundary conditions. The best value of s to fit the data of shear failure of beams and continuous beams (van der Put, 2009) was
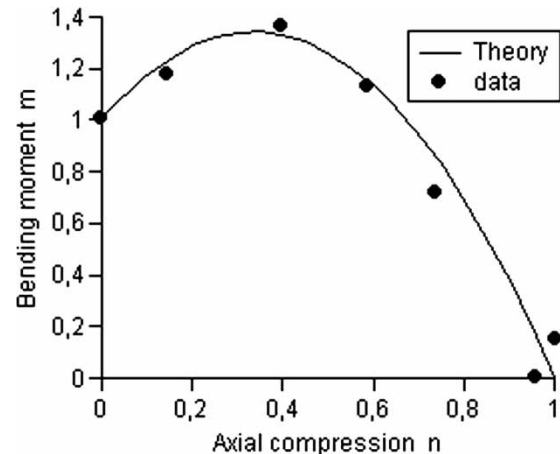

Figure 5. $s = 0.77$ or 5th percentile of the bending–compression strength.

$s = 1.56$ for timber and $s = 2.15$ for veneer wood [laminated veneer lumber (LVL)]. The value of s ($= f_t/f_c$) depends strongly on the wood quality and moisture content.

Because the specimen compression strength f_c and pure tensile strength $f_{t,p}$ (Figure 2) are also measured, the volume effect is directly known. For the 50th percentile it is:

$$s = \frac{f_t}{f_c} = 1.3, \text{ or } \frac{f_t}{f_{t,p}} = 1.3 \frac{f_c}{f_{t,p}} = 1.3 \frac{143}{139} = 1.34 \quad (13)$$

Thus:

$$\frac{f_m}{f_{t,p}} = \frac{3s - 1}{s + 1} \frac{f_c}{f_{t,p}} = \frac{3.9 - 1}{2.3} \frac{f_c}{f_{t,p}} = \frac{2.9}{2.3} \frac{143}{139} = 1.3 \quad (14)$$

For any combination of bending and compression the volume effect factor still is 1.34 (> 1). Here, the proof is given that bending-tension failure always occurs, rejecting the current model of only compression failure by a finite ultimate strain. This applies for any value of s. For the 5th percentile, $s = 0.77$ and $f_t = 1.19\, f_{t,p}$ and $f_m = 1.15\, f_{t,p}$, and for the 95th percentile, $s = 2$ and $f_t = 1.48\, f_{t,p}$ or $f_m = 1.23\, f_{t,p}$. For the Regulations or for design, the failure criterion can be approximated by two lines (eqs 15 and 16) according to the dash–dot lines in Figure 6, intersecting at $n_i = 0.5$, $m_i = 0.5(3s+1)(3s-1)$. Thus:

$$n = 1 - \frac{3s - 1}{3s + 1} m \text{ when } n \geq 0.5 \quad (15)$$

$$m = 1 - \frac{3s - 3}{3s - 1} n \text{ when } n \leq 0.5 \quad (16)$$

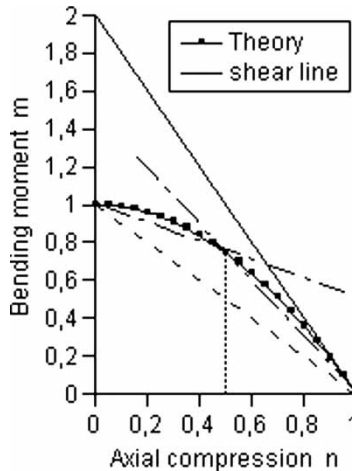At high shear loading, these lines can be cut off by eq. (9): $n = 1 - (3a/h)m$.

Figure 6. Interaction curve cut-off (by the dashed shear line) or no cut-off (by the drawn ultimate shear line).

Shear failure mechanisms are discussed in van der Put (2009). The shear strength V_u here is:

$$V_u = \frac{2}{3} bhf_v = \frac{2}{3} bhf_v' \cdot \left(1 - \frac{x}{h}\right) = \frac{2}{3} bhf_v' \frac{2}{s+1}$$
$$= \frac{2}{3} bhf_v' \frac{2}{2.3} \quad (17)$$

The shear strength is determined by a three-point bending test with a shear slenderness $M_u/V_u h = a/h = 3$. Thus:

$$\frac{M_u}{V_u h} = \frac{f_c(3s - 1)}{8f_v'} = \frac{2.9 f_c}{8f_v'} = 3 \quad (18)$$

giving $f_v' = f_c/8.3$ and $f_v = 2f_v'/(s+1) = 2f_c/(8.3 \cdot 2.3) = f_c/9.5$.

For average wood qualities, the shear slenderness is 3 for failure in shear at the maximum possible bending strength. It then follows from eq. (9) that for $a/h = 3$:

$$n = 1 - (3h/a) \cdot m = 1 - m \quad (19)$$

identical to eq. (6). This is given by the dashed line in Figure 6. Because the shear strength is usually defined by the strength of the three-point bending test with $a/h = 3$, the linear cut-off eq. (6) or (19) applies. To maintain the parabolic failure criterion, the shear strength should be restricted to half its strength value. Then the solid line in Figure 6, $n = 1 - 0.5m$, applies, which does not intersect the parabolic criterion anywhere. Because this shear reduction is not applied in practice and in the Regulations as Eurocode 5, eq. (6) should be applied as the lower bound failure criterion, and for stability design, as proposed by van der Put (1990) for the Eurocode and implemented since then in the Dutch Code. An other reason to apply this straight line is that for high-quality timber such as LVL, $s > 2$, giving the flat curve of Figure 3. This curve flattens more with higher moisture content ($> 14\%$) and moisture content changes and for smaller dimensions (by the size effect).

Bending curvature

The relation for the radius of bending R follows from the maximal elastic stresses of Figure 1. Using eq. (2) with $N = 0$ and eq. (4) the curvature is:

$$\kappa = \frac{1}{R} = \frac{\varepsilon_c + \varepsilon_t}{h - x} = \frac{\varepsilon_c(1 + s)}{h - x} = \frac{f_c(1 + s)}{E(h - x)} = \frac{f_c(1 + s)^2}{2Eh}$$
$$= \frac{2\sigma_m}{Eh} \frac{(1 + s)^2}{4(3s - 1)}$$

$$(20)$$

where $s = \varepsilon_t/\varepsilon_c = \sigma_t/f_c = f_t/f_c$.

To eliminate the varying values of s along the beam, this can be approximated to:

$$\kappa_m = \frac{2\sigma_m}{Eh}\frac{(1+s)^3}{4(3s-1)} = \frac{2\sigma_m}{Eh}\frac{(1+s)^4}{4(3s-1)^2}\frac{\sigma_m}{f_c}$$

$$\approx \frac{2\sigma_m}{Eh}\frac{\sigma_m}{f_c}0.8^{\left(\hat{=}\frac{2\sigma_m}{E'h}\right)} \qquad (21)$$

giving the curvature in the common elastic plastic range. At higher values of s, up to $s = 3$, a mean factor of 0.86 applies according to Table I. In the elastic range it is $\kappa_m = 2\sigma_m/(Eh)$ ($\leq 2f_c/(Eh)$).

Thus, the apparent linear elastic modulus of elasticity E' follows from a reduced modulus by plastic deformation (Figure 7). When the normal force is not zero, the derived curvature becomes:

$$\kappa = \kappa_m/(1 - N/N_u) \qquad (22)$$

Correction of previous approximations

Johns and Buchanan (1982) explained their data of Figure 2 by elastic tension and elastic–plastic compression behaviour. However, a finite ultimate flow strain in compression is assumed to exist and the behaviour therefore remains partly close to elastic, but may also lead to inconsistencies. For instance, when a column fails in pure compression reaching ultimate strain, then rotation of the cross-section is possible, increasing the external moment by the eccentricity of the compression load, while the stress remains fully plastic and the internal moment remains zero. Thus, equilibrium for this assumed failure state is not possible. When a beam fails in pure bending, reaching the ultimate compression strain, then any additional axial loading will decrease the bending tension stress, which remains elastic, and the parameter $s = \sigma_t/f_c$ becomes dependent on the loading and an arbitrary choice of s becomes possible for combined loading. This is demonstrated

Table I. Curvature factor.

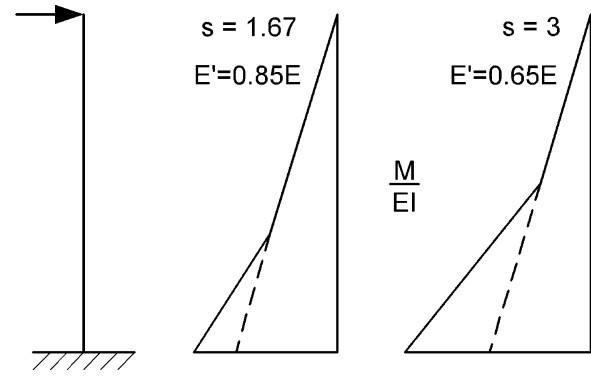| s	$\dfrac{(s+1)^4}{4(3s-1)^2}$
1	1
1.25	0.8
1.5	0.8
1.75	0.8
2	0.8
2.25	0.8
2.5	0.9
2.75	0.9
3	1

Figure 7. Estimation of the reduced modulus of elasticity.

by the limit flow assumption of Blass (1987). In this model, not the mean ultimate stress, but the maximum stress, before the very small yield drop at the start of flow (Figure 8), is chosen as ultimate bending compression stress, limiting the ultimate strain up to this point. Besides the very low ultimate strain, the ultimate stress value is questionable because yield drop is not a material property (van der Put, 1989, 2007), but depends on the rate of loading, temperature, etc., and on the total specimen–testing machine stiffness. It only occurs in a constant strain rate test and thus not in a constant loading rate test or at dead load failure in practice. Further, the moment–curvature diagrams of the model (Figure 8) (of Blass 1987) are also questionable because of the following: (1) A constant ultimate moment cannot exist at an increasing
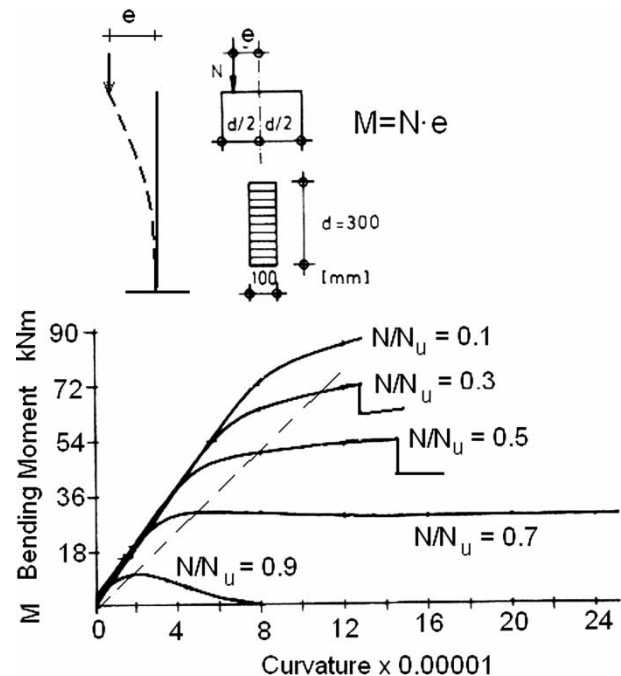

Figure 8. Fictive curvature diagrams (Blass, 1987).

curvature at flow when the normal force ($n = 0.7$) is constant because of the increase in the external moment. (This may only apply for virtual displacements). (2) A decrease in the bending moment at the increase of the curvature is not possible because for a constant loading N, the external moment increases with the increase in deformation and eccentricity, e. Thus, the decrease by yield drop and stepwise decrease in stress at high curvatures in Figure 8 are not possible in a real test (or real simulation) of an eccentric loaded column.

However, the diagrams serve a useful purpose to show the model assumptions made by Blass (1987) for the strength calculation. The dashed line in Figure 8 intersects the chosen ultimate stress points (at the start of the yield drop) for the different values of N, showing that a (non-linear) elastic calculation of the strength is applied that is linearized by the applied secant modulus, where $M/(1 - N/N_u)$ is constant. Extrapolated to pure bending strength $M_{u,0}$ ($N = 0$), the found ultimate load criterion becomes $M/(1 - N/N_u) = M_{u,0}$ or $M/M_{u,0} \approx 1 - N/N_u$, equal to eq. (6). This quasi-elastic solution, based on the start of initial flow, is questionable for real plastic behaviour because it wrongly is based on the linear proportionality of the curvature with the bending stress σ_m, while eq. (21) shows this to be quadratically proportional with σ_m^2. The quasi-elastic equation found by Blass (eq. 6) is therefore far below the strength data and is modified to:

$$\frac{M}{M_{u,fic}} + \frac{N}{N_u} = 1 \qquad (23)$$

where $M_{u,fic}$ is a fictive ultimate bending strength of 60 MPa, to correct the initial flow line to the level of the measurements. This straight interaction line (also found by Johns & Buchanan, 1982) is given in Figure 9 (according to Blass, 1987). For all three cases, seven, 15 and 30 laminations, it is, when extended, the same straight line through 35 MPa compression strength and 60 MPa bending strength. The model thus fails to give the size effect of bending with compression and for pure bending where bending–tension failure is certain. Therefore, because of the size effect, the factorized pure bending strength cannot be 60 MPa for the two (15/7) and four (30/7) times greater depth beams as well. The mean values applied by Blass of the ultimate compression strength (35 MPa) and extrapolated pure bending strength (60 MPa) are deterministic at standard conditions in the applied regression equations, which explains the data lying precisely on a straight line. Not 1000 iterations but one calculation estimates this line of mean values. This also appears to apply for the (adapted?) 5th percentile line because the data are
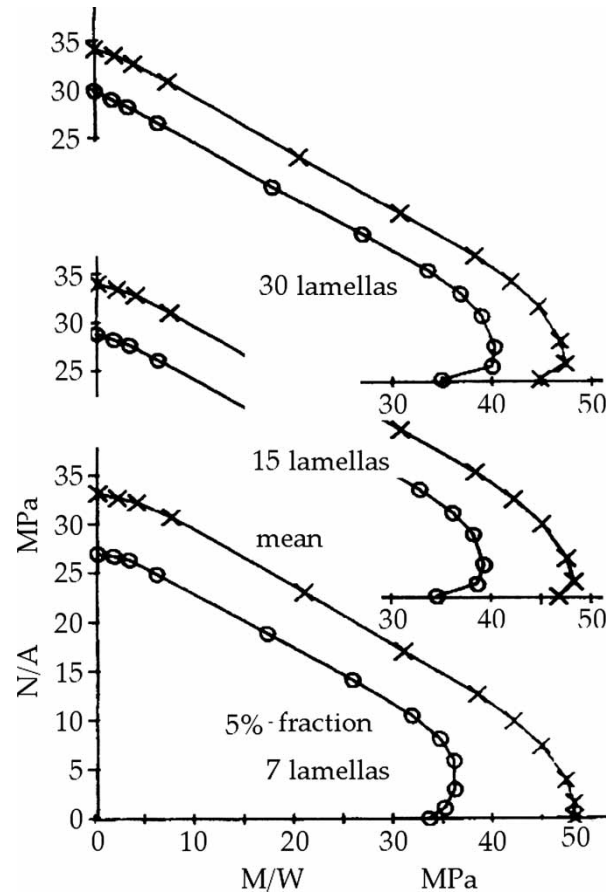

Figure 9. Fictive interaction lines (Blass, 1987).

exactly on the straight line part and do not show, for the 1000 iterations, the still necessary variability around this line.

The empirical eq. (23) can be explained by the theory (eq. 5), leading to $M_{u,fic} = M_{u,a}(1 + 4n/(3s - 1))$, showing that in the Blass model $3s - 1$ is chosen to be proportional to n as an arbitrary loading-dependent ultimate tensile stress condition.

For the pure compression strengths, at the compression axis, a volume effect is suggested to exist, giving in Figure 9 the curved deviations from the straight line near the compression axis of the seven-, 15- and 30-laminate beams. Partly this is due to the change from bending failure to pure compression failure (changing s quickly), but probably is mainly due to following the curve of Johns and Buchanan (1982). This apparent volume effect is explained as follows. The tests of Johns and Buchanan (1982) were performed on two different pieces of test equipment, one for pure compression and the other for combined bending–compression. This caused a small difference between the measured pure compression strength and the extrapolated compression strength from the combined bending–compression test data. This also explains why this assumed (non-existent) volume effect is in the wrong direction.

The departure of Blass (1987) from the straight model line at lower normal loading also follows the fit of Johns and Buchanan (1982) for the seven-laminate beams, suggesting that now the bending–compression strength is no longer regarded as being determining for failure, but rather the bending tensile stress, with $f_m = 48$ MPa instead of the assumed 60 MPa of the straight line of the finite ultimate compression strain model. According to the theory, this leads to $f_m = 48 = f_c(3s-1)/(s+1) = 35 \cdot (3s-1)/(s+1)$, or $s = 1.45$.

However, the value of s is not constant along the curve of Blass and thus does not follow Johns and Buchanan's fit of the data (with $s = 1.3$), but follows their sketched parabolic line, leading to a maximum bending strength at $N = 0$ and thus to the incorrect value of $s = 1.67$ for this failure criterion, which is introduced in the Eurocode. The same applies, for example, for the beam with 30 laminations. This combined compression–bending strength curve is also not based on an ultimate bending tension strength calculation because s never is constant along the curve and is about 1.55 at the top of the curve, reducing to below a value of $s = 1$ when $N = 0$, indicating a very low tensile strength (in disagreement with the applied regression equations). The contrary is to be expected for laminated wood and the real curves therefore can be expected to be flat, like the one in Figure 3.

Because the probability functions of the regression equation, applied by Blass, do not contain a volume parameter and therefore his model cannot account for a size effect, estimation of this effect is necessary. For comparison, the mean tensile strength of the standard laminate is given to be 55.4 MPa, but without specifying dimensions and length belonging to this strength.

The tensile strengths of the simulation model beams with the different bending strength values of about 48, 46.5 and 45 MPa (of Figure 9) can be verified as follows. According to Figure 9, for the beams with seven, 15 and 30 laminations, the coefficient of variation is $v_7 = (48-34)/(1.64 \cdot 48) = 0.178$. Thus, $1/k = 0.3 \cdot 0.178 = 0.0534$. The coefficient of variation is $v_{15} = (46.5-35)/(1.64 \cdot 46.5) = 0.151$. Thus, $1/k = 0.3 \cdot 0.15 = 0.045$. The coefficient of variation is $v_{30} = (45-35)/(1.64 \cdot 45) = 0.136$. Thus, $1/k = 0.3 \cdot 0.136 = 0.0408$. The factor 0.3 follows from the volume effect as follows. Because the bending strength follows from the beam dimension $L/h = 18$, at the same width b, the volume ratio is $18h_1^2 b/18h_2^2 b = h_1^2/h_2^2$ and the strength of the 15-laminate beam with respect to the seven-laminate beam is $(7/15)^{2\alpha v} \cdot 48 = 46.5$, giving $2\alpha = 0.0417/0.15 \approx 10.3$. The same rounded value of α follows from the strength of the 30-laminate beam

with respect to the seven-lamella beam according to $(7/30)^{2\alpha v} \cdot 48 = 45$. This value of α of 0.15 is too low, far below the values found empirically (see Appendix). This leads to the pure tensile strength of the beams with seven, 15 and 30 laminations, respectively, according to eq. (a7) of:

$$f_{t,p} = f_m / \left(\frac{6(k+1)^2}{k+3} \right)^{1/k} = \frac{48}{1.285} = \frac{46.5}{1.25} = \frac{45}{1.22}$$
$$\approx 37 \text{ MPa}$$

Thus, the same tensile strength is predicted for the seven-, 15- and 30-laminate beams, by lack of the size effect in the Blass model. This also follows from eq. (a8) for tests by a constant bending moment loading over the length, giving a tensile strength of 39 MPa in all cases.

The value of $2\alpha = 1.0$ (van der Put, 1977) leads, as a first approximation, to more probable bending strengths with respect to the value of 48 MPa of the seven-laminate beams of $(7/15)^{0.15} \cdot 48 = 42.9$ MPa for the 15-laminate beam and $(7/30)^{0.136} \cdot 48 = 39.4$ MPa for the 30-laminate beam (applying for stable tests).

Conclusions

The assumption of the existing models for combined bending and compression loading, (discussed in the previous section) that a specific compression strain limit is determining for failure is shown to be incorrect. For instance, it predicts from the compression failure that there is no size effect of the strength. The measurements and theory show that there always is a size effect at any value of s and for any load combination because the bending tensile strength is always greater than the pure tension strength of the specimen. For this reason, bending tension failure always occurs, which leads to the starting point of unlimited flow in compression of the plasticity approach modified here.

The derived failure criterion for combined bending with compression is given by eq. (5). This equation can be approximated to two straight lines (eqs 15 and 16), providing simple equations for design and for implementation of the Code.

The derived failure criterion for combined shear with bending and compression is given by eq. (9). Because this line will give a cut-off of the ultimate bending–compression strength lines, this combined shear strength criterion always has to be checked, which should be in the Code.

The size effect is lacking throughout the Blass model, giving questionable predictions of the strengths and an incorrect form of the interaction curves. The parabolic failure criterion of the Johns

and Buchanan and Blass models, applied for Eurocode 5, is unsafe and denies the strong influence of quality and moisture content on the form of the curve (given by the parameter *s*).

The derived equation (eq. 21) shows the curvature along the beam to be a quadratic function of the bending stress σ_m, instead of a linear function of σ_m, as is the incorrect basis of the existing approaches discussed in the previous section. Equation (21) provides a simple method for the ultimate deformation calculation and thus for the ultimate second order bending moment estimation.

References

Blass, H. J. (1987). *Tragfähigkeit von Druckstäben aus Brettschichtholz unter berücksichtigung streuender Einflussgrössen.* Thesis, University of Karlsruhe. (See also CIB-W18/19-12-2 and CIB-W18/20-2-2.)

Chen, W. F. & Atsuta, T (1977). *Theory of beam-columns. Vol.2: Space behaviour and design.* New York: McGraw-Hill.

Eurocode 5 (2004). *EN 1995-1-1 Design of timber structures, Part 1-1: General—Common rules and rules for buildings.* Technical committee CEN/TC50 Structural Eurocode, Secretariat BSI.

Johns, K. C. & Buchanan, A. H. (1982). Strength of timber members in combined bending and axial loading. *CIB/IUFRO Meeting*, Boras, Sweden. (See also CIB-W18, 1985, Israel.)

van der Put, T. A. C. M. (1977). *Influence of specimen dimensions on strength properties of glulam* (Rep. 4-77-5 he-7). Delft: Stevin Laboratory, Delft University. (In Dutch.)

van der Put, T. A. C. M. (1981). *Finger-joints in glulam* (Rep. 4-81-5 VL-3). Delft: Stevin Laboratory, Delft University. (In Dutch.)

van der Put, T. A. C. M. (1989). *Deformation and damage processes in wood.* Delft: Delft University Press.

van der Put, T. A. C. M. (1990). *Stability design and code rules for straight timber beams.* Meeting CIB-W18/23-15-2.

van der Put, T. A. C. M. (2007). Softening behaviour and correction of the fracture energy. *Theoretical and Applied Fracture Mechanics*, 48, 127–139.

van der Put, T. A. C. M. (2009). Derivation of the shear strength of continuous beams. *Holz als Roh Werkst* (accepted).

Appendix: Size effect

The influence of the size effect always has to be regarded in strength calculations. For the general applicability a simple derivation of the size effect is given in the following.

The survival probability of a specimen with volume *V*, loaded by a constant tensile stress σ, as in the standard tensile test, can be given as function of the stress by:

$$P_s(V) = \exp\left(-\frac{V}{V_0}\left(\frac{\sigma}{\sigma_0}\right)^k\right) \tag{a1}$$

because the power law may represent any function of σ around a stress value.

For a stress distribution eq. (a1) becomes:

$$P_s(V) = \exp\left(-\int_V \left(\frac{\sigma(x,y,z)}{\sigma_0}\right)^k dx \cdot dy \cdot dz/V_0\right) \tag{a2}$$

This specimen has an equal probability of survival as the standard test specimen eq. (a1) when the exponents are equal, thus when:

$$\int_V \left(\frac{\sigma(x,y,z)}{\sigma_0}\right)^k dV = \left(\frac{\sigma_s}{\sigma_0}\right)^k V_s \tag{a3}$$

For the stress distribution, $\sigma = \sigma_b(1-2y/h)(1-x/a)$, according to Figure 10, is:

$$\int_V \left(\frac{\sigma(x,y,z)}{\sigma_0}\right)^k dxdydz = \frac{ahb}{2}\int\int\left(\frac{\sigma_b}{\sigma_0}\left(1-\frac{2y}{h}\right)\left(1-\frac{x}{a}\right)\right)^k \frac{dx}{a}\frac{dy2}{h}$$

$$= \frac{ahb}{2(1+k)^2}\left(\frac{\sigma_b}{\sigma_0}\right)^k \tag{a4}$$

For the three-point bending test this is twice as high. For the middle part of the four-point bending test specimen, by the constant moment:

$$\int_V \left(\frac{\sigma(x,y,z)}{\sigma_0}\right)^k dxdydz = \frac{ahb}{2}\int\int\left(\frac{\sigma_b}{\sigma_0}\left(1-\frac{2y}{h}\right)\right)^k \frac{dy2}{h}$$

$$= \frac{ahb}{2(1+k)}\left(\frac{\sigma_b}{\sigma_0}\right)^k \tag{a5}$$

Thus, for the four-point bending test:

$$\int_V \left(\frac{\sigma(x,y,z)}{\sigma_0}\right)^k dxdydz = \left(\frac{\sigma_b}{\sigma_0}\right)^k \left(\frac{Lbh}{3(1+k)^2}+\frac{Lbh}{6(1+k)}\right)$$

$$= \left(\frac{\sigma_b}{\sigma_0}\right)^k \frac{V(k+3)}{6(k+1)^2} \tag{a6}$$

where $L=3a$ is the length of the specimen.

According to eqs (a3) and (a6), the bending strength of the bending tests is:

$$\frac{\sigma_{b,4}}{\sigma_s} = \left(\frac{6(k+1)^2}{k+3}\frac{V_s}{V_b}\right)^{1/k} = \left(\frac{6(k+1)^2}{k+3}1.25\right)^{1/k} = \frac{f_m}{f_{t,p}} \tag{a7}$$

where $V_s/V_b = L_s/L_b$, the length ratio, because for all specimens *bh* is the same and $L_s/L_b = 3/2.4 = 1.25$ (tests of Johns & Buchanan, 1982) in this case.

The 900 mm specimens of the compression–bending tests were loaded by eccentrical compression and thus by a constant moment along the length. According to eqs (a3) and (a5) the bending strength (for zero compression) is:

$$\frac{\sigma_b}{\sigma_s} = \left(2(k+1)\frac{V_s}{V_b}\right)^{1/k} = (2(k+1)3.33)^{1/k} = \frac{f_m}{f_{t,p}} \tag{a8}$$

because now $V_s/V_b = L_s/L_b = 3/0.9 = 3.33$. The nominal length of the pure tension test specimen was $L_s = 3$ m (Johns & Buchanan, 1982). The value of k is 5–10 for timber, depending on the coefficient of variation. For $k=5$, $f_m/f_{t,p} \approx 2.05$, according to both eqs (a7) and (a8). For $k=10$, both equations give $f_m/f_{t,p} \approx 1.54$.
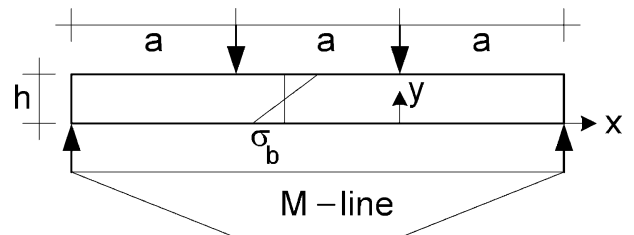

Figure 10. Four-point bending test.

For glulam $k = 20$ is possible and both equations give $f_m/f_{t,p} \approx 1.28$. This means that the bending strength, measured in the four-point bending test, also applies for the 0.9 m short compression specimens, loaded by a constant moment.

In the derivation above the linearized bending strength is used. This is possible because the triangle tensile stress area of the real elastic–plastic stress distribution in Figure 1 is about equal to that of the linear stress distribution (the dashed line in Figure 1). This is verified by tests of van der Put (1981), where in this way $f_m/f_{t,p} \approx 1.27$ was predicted and measured in the four-point bending test, while $f_m/f_{t,p} \approx 2.3$ was predicted and 2.2 was measured in the three-point bending test.

The discussion of the volume effect for combined bending with tension is not discussed in this article. For low tension, the equations are the same as for compression, with an opposite sign for the uniform tensile stress. For high tension the calculation is according to the theory of elasticity as discussed by Johns and Buchanan (1982).

The Weibull constant k for brittle failure is given by eq. (a9):

$$v^2 = \frac{\Gamma(1 + 2/k)}{\Gamma^2(1 + 1/k)} - 1 \tag{a9}$$

where v is the coefficient of variation. Expansion of the gamma functions shows that $k = f(v)/v \approx 1.2/v$, where $f(v)$ is a little varying function around a value of about 1.2 in the range of common applications. For less brittle failures, as in wood, it is shown (van der Put, 1971) for specimens of the same form and loading that:

$$\frac{\sigma}{\sigma_1} = \left(\frac{V_1}{V}\right)^{\alpha v} \quad \text{and} \quad \frac{v}{v_1} = \left(\frac{V_1}{V}\right)^{\beta} \tag{a10}$$

where $0.83 \geq \alpha \geq 0$ and $0 \geq \beta \geq 0.5$, where $(\alpha, \beta) = (0.83, 0)$ is brittle and $(\alpha, \beta) = (0, 0.5)$ is fully plastic behaviour. For common tests and large samples of glulam $\alpha v = 0.1$. This also depends on the species and is, for example, $\alpha v = 0.05$ for southern pine (AITC Technical Note 21). Thus, $\alpha \approx 1/3$ to 2/3. Stable material property tests of glulam showed for the brittle failure types such as tension, splitting and shear of European glulam, $\alpha = 0.5$ (van der Put, 1971) was a better value than $\alpha = 0.15$ assumed by Blass (1987). The value of β is about 0.2.